Element-specific magnetization of a Gd-Co composite system using spin-polarized Auger electron spectroscopy

O. S. Anilturk* and A. R. Koymen
The University of Texas at Arlington (UTA), Physics Department, P.O. Box 19059, Arlington, Texas 78721, USA
(Received 7 January 2003; published 31 July 2003)

Spin-polarized Auger electron spectroscopy is found to have applications for monitoring element-specific magnetization in composite systems. Here, we report on an application of such a study performed on a Gd-Co composite system. Special emphasis is given for $4d$-core-hole-initiated Auger decays in Gd interacting with a Co subnetwork within the energy region of 30–150 eV. Prominent resonant ($4d \rightarrow 4f$) and nonresonant Auger lines involving $4d(N_{45})$, $5s(O_1)$, $5p(O_{23})$, $4f(N_{45})$, and $(5d,6s)(V)$ valence states are identified with the information obtained on either the spin polarization spectrum or the corresponding Auger spectra. Besides the applicability of this technique in this system, it is observed that the $5d$ states have enhanced spin polarization, confirming the coupling of moments in the composite system via $5d$ states of gadolinium. It is also directly observed that Co magnetic moments are indeed aligned antiparallel to the Gd ones, as has been postulated by theory and indirectly determined by various methods.

DOI: 10.1103/PhysRevB.68.024430 PACS number(s): 75.70.Rf, 75.25.+z, 75.60.Ch, 79.20.Fv

INTRODUCTION

Because amorphous rare earth and transition metal (RE-TM) alloys are commonly used as the storage layer in magneto-optical storage media,[1] their magnetic properties have been extensively investigated. An important characteristic of RE-TM systems is that they exhibit ferrimagnetism in which the RE moments are aligned oppositely to TM moments.[2] In the case of Gd with Co, it is reported that the alignment is purely collinear.[3,4] This behavior makes the Gd-Co alloy an ideal and interesting case to study the fundamental coupling between the two sublattice structures.

Gd is the most interesting member of the lanthanide series in that its ground-state electronic configuration is $4f^7(5d6s)^3$ with the highest possible number of majority-spin electrons and no minority-spin electron at its $4f$ state according to Hund's rule. For the low-energy portion of up to 150 eV, the Auger electron spectrum on Gd exhibits several structures due to Coster-Kronig (CK) transitions with the different shell electrons and to the super-Coster-Kronig (sCK) transitions with the same shell electrons. Besides these transitions involving $4d(N_{45})$, $5s(O_1)$, $5p(O_{23})$, $4f(N_{45})$, and $(5d,6s)(V)$ valence states, it is found that the direct recombination (DR), or so-called ''giant resonance,'' with the initial state of the $4d^9 4f^8$ resonant transition is the most dominant mechanism to the high-energy region of the spectra up to $4d$ absorption threshold ($\sim$142 eV). Decay channels following the resonant $4d \rightarrow 4f$ transition have been studied extensively by several authors for Gd (Refs. 5–9 and 12–14) with both photon and electron-excited core-hole generation methods. Of the Auger electron spectrum studies, after the first observation of the direct recombination ($4d \rightarrow 4f$) process by Dufour and Bonelle,[5] Gerken *et al.*[6] identified several structures in the spectra of Gd as due to $4d \rightarrow 4f$ direct recombination. The most intensive work was done by Riviere *et al.*[7] who studied a complete set of electron-excited Auger spectra of lanthanides with $4d$-core-hole-initiated processes. In their work, they also studied the transition rates for different decays by including the effect of spin alignment resulting from strong coupling in the initially unfilled shells. Energy losses related to the $4d$ level together with the Auger spectrum were analyzed by Kolaczkiewicz and Bauer.[8] Synchrotron radiation studies involving decay channels of the $4d$ core hole were done by Sarma *et al.*[9] The spin polarization consideration of the generated electrons has been given in some of these studies at the specific energy range of the spectrum. On the other hand, the spin-polarized Auger electron study of Taborelli *et al.*[10] has been hitherto the one and only electron-excited experimental work on pure Gd in the literature, besides the pioneering studies of fundamental magnetic materials (Fe, Ni) of Allenspach *et al.*[11]

Spin-resolved studies constitute the most directly accessible and crucial way to investigate the coupling of Gd with the TM system. Most of the spin-resolved studies are performed on Gd-Fe bilayer systems. Magnetic ordering of very thin Gd layers on Fe was studied by Taborelli *et al.*,[12] in which they concluded the antiferromagnetic coupling of two sublattices with spin-polarized Auger electron spectroscopy. The spin polarization study of this bilayer system by Taborelli *et al.*[12] is then followed by Carbone and Kisker[13] and Kachel *et al.*[14] in which Gd overlayer structures on Fe(100) are studied by photoemission spectroscopy with considerations given to the Gd electron spin polarization at specific levels.

In this study, we have performed spin-polarized Auger electron spectroscopy (SPAES) on Gd-Co with special emphasis given to Gd in the alloy system; therefore, element-specific information on Gd is achieved. Various considerations of the obtained spectra are given in detail.

EXPERIMENTAL PROCEDURE

Reviews of both SEMPA (scanning electron microscopy with polarization analysis) and SPAES are described elsewhere in the literature.[15,16] Our SEMPA system has also been introduced in previous studies of 3% Si-Fe (Ref. 17) and Permalloy films (Ref. 18). However, a brief description of

the technique for extraction of spin-polarized Auger spectra will be given in this paper.

Under ultrahigh-vacuum conditions with a base pressure of $<2-3\times10^{-10}$ Torr, the magnetic sample is irradiated by an energetic electron beam of 8 keV. The system uses a compact Mott spin polarimeter, operated at 25 kV with a passivated Th foil, which has been attached to the back of a hemispherical energy analyzer (HSA). The excited secondary electrons are transported using electrostatic optics and are energy selected by the energy analyzer. The energy resolution of the analyzer is $\Delta E/E=0.5\%$, and the probe diameter of the beam is around 0.2 μm.[17] Subsequently, after energy analysis, the secondary electrons are scattered by the Th foil to four channel electron multipliers (CEMs). Therefore, at a specific energy window of the HSA, the relative in-plane angular variation $[\theta=\tan^{-1}(P_y/P_x)]$ and the magnitude of polarization $(P=\sqrt{P_x^2+P_y^2})$ can be extracted by using the two measured orthogonal in-plane components of the magnetization. A Ag foil is attached to the same sample stub used for the magnetic sample, thus allowing the removal of any instrumental asymmetries *in situ*. Both the Ag foil and magnetic sample were ion sputtered with a 1.5-keV Ar^+ beam.

Two schemes of data collection procedure are applied to obtain microscopic and spectroscopic information. In the domain-imaging mode, the energy window of the energy analyzer is set to the secondary electron emission peak, and then the beam is scanned on the sample to obtain the picture of the domain structure with desired magnification. While in the SPAES mode, the energy window is altered successively for the whole spectrum in a desired energy range in order to obtain the spin polarization at each energy value of the energy analyzer at a particular region or domain of the sample. This is the main advantage of the UTA-SEMPA system. In previous SPAES studies, the same spectroscopic information was obtained by averaging two consecutive measurements with opposite sample magnetization, thus disturbing the magnetic system, to eliminate any asymmetries due to the apparatus as well as to the spin-orbit coupling in the electron scattering processes. However, in the present system, the single-domain state is obvious by the observed domain structure at hand. Furthermore, the need for two measurements is eliminated by the removal of the instrumental asymmetry using a Ag foil. Another question may arise for the asymmetry due to the spin-orbit coupling in the scattering processes; however, this investigation is the scope of another study.

Since the secondary-electron cascade includes both Auger and true secondary electrons, Auger spectrum leading to spin polarization information should be extracted from this cascade. At first glance, the most appropriate way seems to be using an analytical expression to approximate the secondary-electron distribution and numerically remove the secondary-electron distribution from each spectra obtained in the four channeltrons. For this purpose, a Ramaker function, given in the following equation,[19] has been fitted to the tail of the four spectra in each CEM:

$$N_{Ramaker}=A\left(\frac{E}{(E+E_0)}\right)(E+\phi)^m + B\left(\frac{EE_p}{(E_p-E)}\right)^n \ln\left(\frac{(E_p-E)}{E_p}\right)+C,$$

where A, B, C, m, n are constants, E is the energy of the electron, E_p is the energy of the primary electron beam, E_0 is the escape probability parameter, and ϕ is the work function of the material. As an extension to the Sickafus function,[20] the Ramaker function is a more sophisticated background function, which includes the effects of backscattered electrons at the energy tail of the secondary-electron spectrum. The polarization values are then calculated from the background subtracted spectra of each counter. In the following, the described procedure is applied to extract polarization information within the energy intervals of different Auger structures. Although the background subtraction induces large uncertainties ($\sim$15%) in the spin polarization values, the qualitative information given here is unchanged by this procedure.

A 1250-Å-thick Gd-Co alloy sample was codeposited from Co and Gd targets on a glass substrate (Corning 7039) by power-mode-controlled dc magnetron sputtering. The concentration of Gd in the composite system is 25%–30%. Deposition was done in a UHV chamber with unbaked base pressure of 6×10^{-9} Torr at room temperature. Deposition pressure was 3 mTorr and ultrahigh-purity Ar gas was used.

The hysteresis loop of the sample is square and shows in plane magnetization. The sample was demagnetized by performing consecutive hysteresis loops such that the magnetic field was reduced in each consecutive hysteresis. The surface magnetic domain structure of the film is obtained in SEMPA mode. Then, SPAES measurements are performed on one of the domains by making sure that the region being probed is a single domain with SEMPA measurements.

RESULTS AND DISCUSSION

In Figs. 1(a)–1(d), our results obtained on a Gd-Co sample at room temperature are presented for the energy region of both M_xVV $(x=1,23)$ transitions for cobalt, and $N_{45}XY$ $(X,Y=4d,5p,5s,4f,V)$ transitions together with resonantly excited Auger transitions for Gd. These results are obtained after successive intensity background subtractions to each spectrum obtained on four channeltrons at the shown energy region, as described before. The intensity spectra shown in Fig. 1(a) present distinct features that are less complex compared to their polarization counterpart. However, it is the scope of this study to describe the involved transitions with the results obtained on the spin polarization spectrum. In Fig. 1(a), going from the low- to high-energy tail of the spectra, the first prominent peak is the $M_{23}M_{45}M_{45}$ normal Auger line of Co, which is dominated by the $3d$ electron excitation of another $3d$ electron relaxation to the ionized $3p$ state of Co. Its spin polarization reflects the $3d$-band polarization of Co. This effective polarization value is obtained to be $\sim$50%, which is higher than the obtained value of the effective polarization of 24% in a separate study performed on polycrystalline cobalt film.[21] The polarization difference is attributed to the effect of alignment, due to local anisotropy, of local Co magnetic moments in the current alloy system. Above the $3p$ threshold of Co, up to $\sim$80 eV, several structures are seen in the polarization spectra which is supported by very weak intensity structures at the higher-

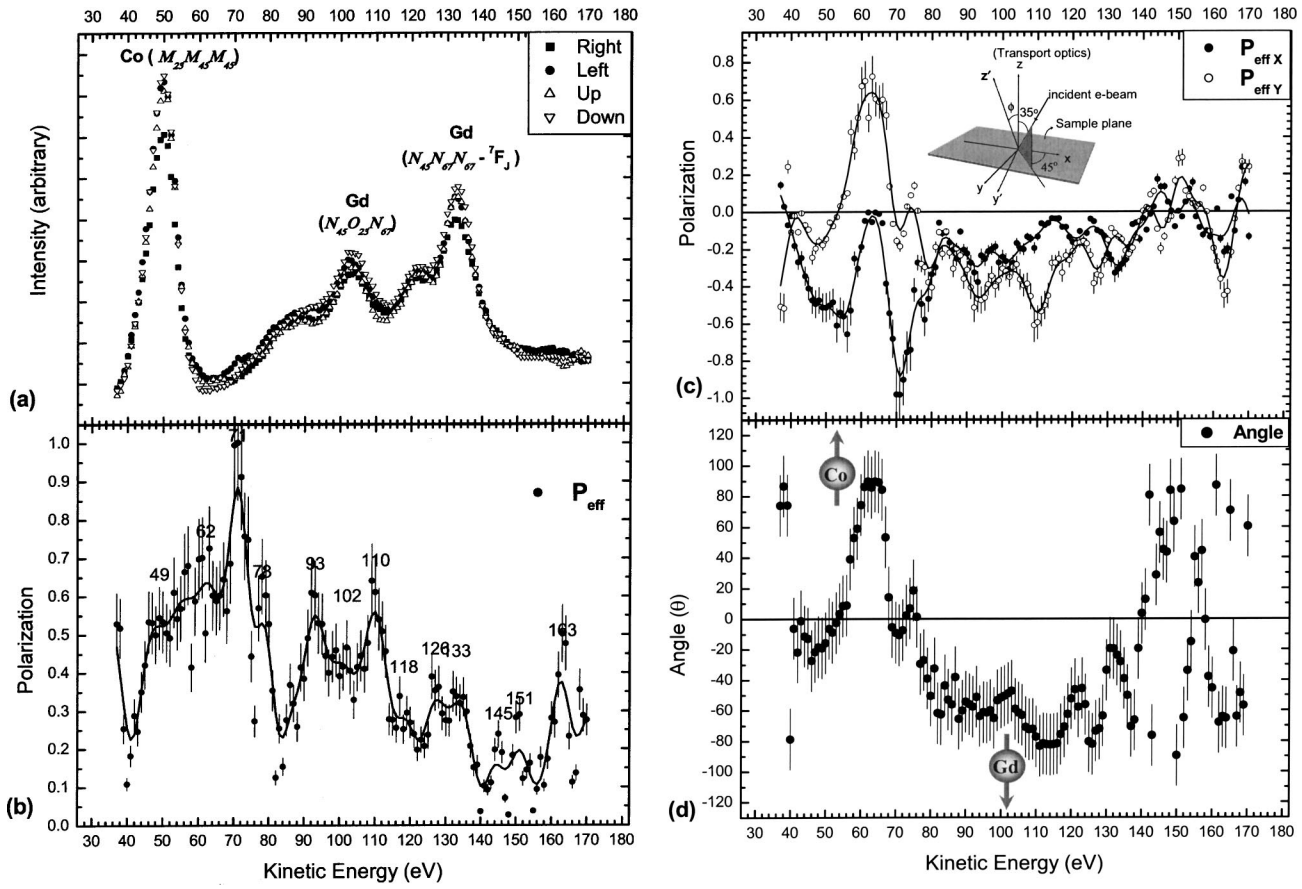

FIG. 1. (a) Intensity spectra obtained at four channeltrons of the polarimeter after successive background subtractions. The designations of the channeltrons are given as viewed normal to the scatterer plane. (b) Auger spin polarization spectrum of Gd-Co composite system in the energy region of M_xVV ($x=1,23$) transitions for Co and $N_{45}XY$ ($X,Y=4d,5p,5s,4f,V$) transitions for Gd. The black line is three-point fast Fourier transform (FFT) smoothing of the data, drawn as a guide. (c) X and Y components of the polarization constituting the spin polarization spectrum. The inset shows the sample geometry with respect to the transport optics. (d) Angle variation corresponding to the polarization spectrum in (a). The representative Co and Gd moments are drawn in the inset, not necessarily residing at exact energy region.

energy tail of the main Co Auger line. It is known that some of these structures are related to autoionization emission of resonant $3p$-$3d$ excitation in $3d$ transition metals,[16,21,22] which are expected to have higher spin polarization, because of the availability of only minority states at the $3d$ band. The intensity spectra in Fig. 1(a) then show very distinct features, which are related mostly to Auger decay channels of ionized $4d(N_{45})$ states of gadolinium predominantly determined by the resonant $4d\rightarrow 4f$ excitation. The most important decay channels of resonant $4d\rightarrow 4f$ excitation, and CK and SCK Auger transitions including their possible spin configurations, are shown in Figs. 2(a)–2(d). In the figure, only $4d$-core-hole-initiated transitions are shown, since these transitions fall into the energy range of interest. Alternatively, an Auger transition of the kind $3d4dX$, where X stands for any state from $4d$ to V, may also result in a $4d$ core hole at high enough primary electron energies. This is indeed the case for the energy of the primary electron beam used in the experiment as follows: The relative contribution of $3d$ and $4d$ levels on the basis of relative ionization cross sections can be estimated as[23]

$$\frac{P(3d)}{P(4d)} \approx \frac{E(4d)}{E(3d)} \frac{n(3d)}{n(4d)} \frac{\left\{1+\frac{2}{3}\ln\left(\frac{E_P}{E_B(3d)}\right)\right\}}{\left\{1+\frac{2}{3}\ln\left(\frac{E_P}{E_B(4d)}\right)\right\}},$$

where P's are the probabilities of ionization, E_B's and n's are the corresponding binding energies and number of electrons, respectively, and E_P is the primary beam energy. Thus, for 8 keV beam energy, it is calculated that the probability of $3d$ ionization is 87% of that of $4d$ ionization. Therefore, it is probable that a $4d$ core-hole generation may also be the result of a $3d4dX$ Auger transition. However, energetically, these transitions will be off the energy range and will only assist in $4d$ core-hole generation.

Of the structures in the spectra in Fig. 1(a), the distinct intensity structure at 102 eV is the $N_{45}O_{23}N_{67}$ transition that is also of the strongest Auger processes that contribute significantly to the intensity structure. In these processes, there is no spin preference of O state ($5p$ or $5s$) electrons to fill the $4d$ core hole. As is shown in Fig. 2(d) ($d5$ and $d6$), one

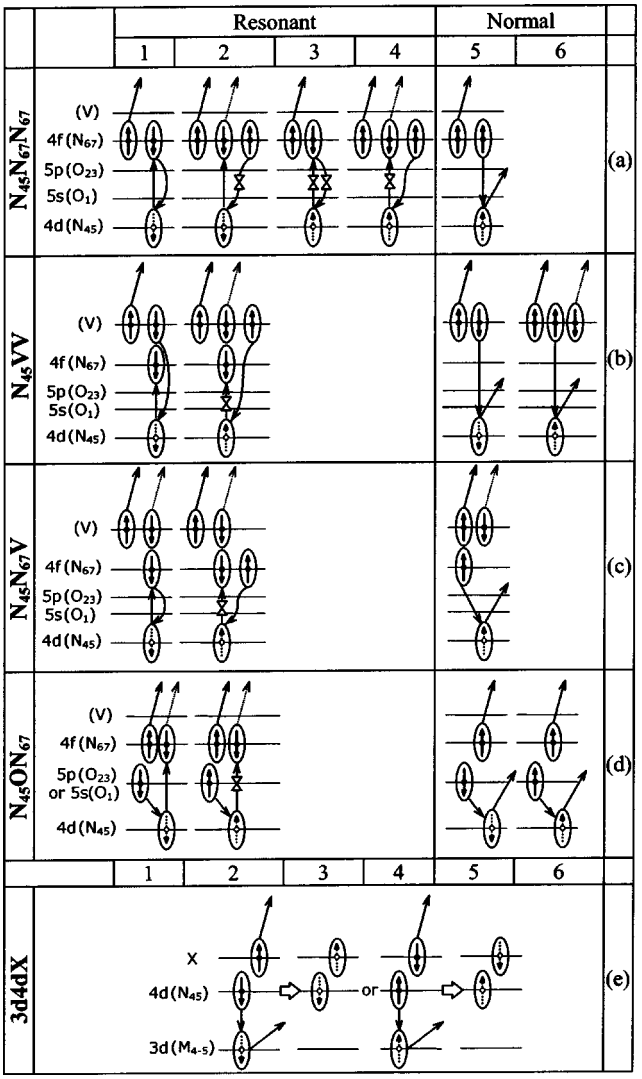

FIG. 2. (a)–(d) The schematic picture of representative $4d$-core-hole-initiated resonant (*left*) and normal (*right*) Auger transitions of gadolinium, explained in the text. (e) Representation of $4d$ core-hole generation via a $3d$-$4dX$ Auger transition. The transitions involving spin-flip processes in excitation and/or relaxation are shown as double triangles.

would expect this sharp structure as one of the dominant processes after core-hole creation at $4d$, since there exists no restriction on the creation and relaxation involving the two states. One would expect high spin polarization as a result of these transitions, because the Auger electron is from the fully polarized $4f$ level if no charge transfer is involved. This is indeed the case with $\sim$45% in our polarization spectrum. The rather broad shoulder of this structure towards the lower-energy region that peaks around $\sim$88 eV is attributed to collective contribution of $M_1M_{45}M_{45}$ of Co and two Auger structures: namely, $N_{45}O_{23}O_{23}$ and $N_{45}O_1V$ of Gd. The former transition in Gd, $N_{45}O_{23}O_{23}$, tends to decrease the spin polarization at the middle of this broad peak, and the latter, $N_{45}O_1V$, gives rise to spin polarization due to the nature of the valence band in Gd. The peak polarization at $\sim$93 eV is due to the latter transition. As we will discuss in the following, it is observed that the polarization arising from the transitions including the valence band ($5d^16s^2$) is in general higher than the counterpart, which involves the $4f$ level of Gd. This is indeed the case for the polarization peak observed also at 110 eV, which is assigned to the $N_{45}O_{23}V$ transition. The spin polarizations of both structures are found to be around 60%, which validates the self-consistency of the polarization spectrum. The observed enhancement of the valence-band polarization of Gd arises from the coupling of Co to Gd moments via the $5d$ states.

At the energy region of 115–145 eV, two other features at 123 eV and 133 eV are visible in the spectra shown in Fig. 1(a). Of these structures, the broader peak at 123 eV is composed of multiple structures of resonantly and nonresonantly excited Auger decays of $N_{45}N_{67}X$ ($X=N_{67}$, V) transitions. The normal Auger line $N_{45}N_{67}N_{67}$ [Fig. 2(a5)] of these transitions with a $4f^{-2}$ two-hole final state is expected to be at the lower-energy tail of this broad peak. Although the intensity feature associated with this transition is not readily seen in the intensity spectra, the polarization spectrum reveals this structure with a polarization peak around 118 eV with a peak value of $\sim$30%. This value is not consistent with the one obtained from the $N_{45}O_{23}N_{67}$ transition (45%), and the difference is attributed to the respective difference in recombination channels of $5p$-$4d$ and $4f$-$4d$ states [see Figs. 2(a5) and 2(d5), (d6)]. The second assignment from the polarization spectrum is the peak structure at 126 eV with a polarization of $\sim$35%. This structure is the combination of two transitions: namely, resonantly excited $N_{45}N_{67}N_{67}$ (^5X_J) and normal $N_{45}N_{67}V$ transitions [Fig. 2(c)], where X stands for all possible angular momentum quantum numbers.[6] As is shown in Fig. 2(a), $N_{45}N_{67}N_{67}$ Auger transitions after resonant $4d\rightarrow 4f$ excitation [(a1)–(a4)] with $4f^{-1}$ single-hole final state are shown. Of the resonant excitation processes, all processes require the spin-flip scenario at some stage of the transition, either excitation or decay, or both, except for the excitation of a spin-down electron (a1) to the available minority spin state at the $4f$ level. In a recent photoemission study[24] of spin-flip processes involving $4d-4f$ transitions, it is suggested that the spin flip predominantly takes place in the photoexcitation stage. Therefore, we assume that only the processes of type (a3) and (a4) dominate the spin-flip-involved transitions. As can be clearly visualized with the simplest picture, this process may lower the spin polarization of the Auger electrons originating from this resonant $N_{45}N_{67}N_{67}$ transition. The transition (^7F_J) in Fig. 2(a1), which does not involve the spin-flip process, obeys spin conservation. This transition dominates the high-energy region of the intensity spectra by a sharp peak at 133 eV and has polarization value of 33%. For the sake of completeness, it should also be noted that the $4d$ core hole may result from the ionization of a spin-down electron, but the decay of any electron from the $4f$ level is spin prohibited, not shown in Fig. 2(a).

At the resonant and nonresonant regions of the polarization spectrum, the polarization values are seen to be lowered by around 30% between 115 and 140 eV, compared to its counterpart with $5p$-$4d$ relaxation. This can be safely attributed to the spin-flip contribution of the resonant process,

TABLE I. The observed spin polarization values of prominent Auger lines (in %). The data at last column are for comparison of the polarization values obtained on Gd-only sample by Taborelli *et al.* (Ref. 10). Expected energies are due to Riviere *et al.* (Ref. 7).

Transition	Expected energy[a]	Energy	Polarization (%)	Peff (%)[b] at 2.5 keV
$N_{45}O_1V$	99	93	60	
$N_{45}O_{23}N_{67}$	111	102	45	24
$N_{45}O_{23}V$	120	110	60	
$N_{45}N_{67}N_{67}(^7D_J)$	126	118	30	28
$N_{45}N_{67}N_{67}(^5X_J)$	134	126	35	31
$N_{45}N_{67}V$				
$N_{45}N_{67}N_{67}(^7F_J)$	140	133	33	42
$N_{45}VV$				

[a]Reference 7.

[b]Reference 10.

which is predicted to be about 30% by the calculation of Sugar[25] on trivalent Gd atoms. Therefore, a 30% reduction in polarization values, including the spin-flip contribution, the $4f$ level polarization of 30% is an important point for the consistency of the experiment. As was mentioned previously, the excitation source of a 8-keV electron beam assists the promotion of $3d$ core holes. It is known[9] that the normal Auger line of the kind $N_{45}N_{67}N_{67}$ is strongly affected by the presence of spectator-hole satellites at high energies, relative to $N_{45}O_{23}N_{67}$ transitions.

Auger transitions, namely, $N_{45}VV$, involving the $5d^16s^2$ valence (V) states with initial state of either $4d$-$4f$ resonant excitation or $4d$ electron ionization, are shown in Fig. 2(b). The normal Auger line of this transition Fig. 2(b4) and 2(b5) may contribute to the structure observed at 133 eV. Observed structures both in intensity and polarization spectra are tabulated in Table I.

Following the above discussion of uniquely observed fine structures of both intensity and polarization spectra, in Figs. 1(c) and 1(d), the spectra of two orthogonal polarization components, namely, P_x and P_y, and the angular variation of the polarization are shown, respectively. The angular variation of the polarization unambiguously shows the coupling between two subnetworks within the composite system. For the Co region of the angle spectrum in Fig. 1(d), the polarization arises from the admixture of majority electrons with the minority electrons of Co sites between 40 and 56 eV, thus zero degree. Then, there exist resonantly emitted dominant majority electrons of cobalt between 57 and 70 eV pointing upwards: from this point forward, the spectra are dominated by Gd Auger electrons, especially from $4f$ and $5d$ states pointing downwards. The details of all spectra, including the angle variation spectrum, also show effects of configuration interactions in the system, which is valuable for theoretical aspects.

As was explained in the text, the determination of $4f$ and $5d$ level polarization values of Gd makes the comparison with previous available data possible. The effective spin polarization value of the $4f$ level is expected to be 100%, assuming spin conservation. In previous studies[12–14] performed on bilayer systems of Gd-Fe, the $4f$ spin polarization is found to have a dependence on both the thickness of the Gd adlayer and the temperature. At $T=170$ K, Carbone and Kisker[13] found a value of 60% for $4f$ level polarization on the 1-ML Gd/Fe(100) system. The room-temperature measurement by Kachel *et al.*[14] showed a value of $\sim$45% polarization of the $4f$ level from both on- and off-resonance photoemission experiments on the same system. Although in an alloy with cobalt, the $N_{45}O_{23}N_{67}$ normal Auger line probing the $4f$ level of Gd shows excellent agreement with previous studies. This transition is relatively more important from theoretical aspects as being the undisturbed Auger line of core levels only of Gd. From our measurements, the spin polarization value of this normal line is found to be also 45%, which is very consistent with the previous work.

The spin polarization of the $5d$ state in Gd is found to be rather strong (60%), as it is the state that translates the moment distribution between Gd $4f$ and Co $3d$ states via $3d$-$5d$ hybridization. Strong polarization with the same orientation of Gd $4f$ states confirms that the $5d$ states are ferromagnetically aligned with the Gd $4f$. The spin polarization value given here is valuable information about the RE-RE and RE-TM exchange interactions. It also confirms that the coupling is mediated by the $5d$ state via the $4f$-$5d$ exchange and the $3d$-$5d$ hybridization, as was expected from the molecular orbital formalism.[2]

In conclusion, we have performed spin-polarized Auger electron spectroscopy on the Gd-Co composite system. Details of the $4d$-core-hole-initiated Auger transitions including their spin polarization and energetics are given. The $4f$ polarization values of Gd are seen to be coherent and very consistent with previous studies performed on bilayer systems. Besides the element-specific information obtained both for Co and Gd, it is observed that the $5d$ states have enhanced spin polarization, confirming the coupling of moments in the composite system via $5d$ states of Gd. It is also unambiguously observed that Co magnetic moments are indeed ferrimagnetically aligned to the Gd ones via $4f$-$5d$ positive exchange and $3d$-$5d$ hybridization. We hope that the information obtained here will serve as another data point obtained for understanding of fundamental properties of RE-TM systems.

ACKNOWLEDGMENTS

The authors would like to thank Dr. Baki Altuncevahir for the sample preparation and stimulating discussions. This research was supported by the Welch Foundation.

*Electronic address: Onder.Anilturk@motorola.com

[1] J. Daval and B. Bechevet, J. Magn. Magn. Mater. **129**, 98 (1994).
[2] M. S. S. Brooks, L. Nordstrom, and B. Johansson, J. Phys.: Condens. Matter **3**, 2357 (1991).
[3] See, for example, S. Uchiyama, Mater. Chem. Phys. **42**, 38 (1995).
[4] T. Iwazumi, T. Nakamura, H. Shoji, K. Kobayashi, S. Kishimoto, R. Katano, Y. Isozumi, and S. Nanao, J. Phys. Chem. Solids **61**, 453 (2000).
[5] G. Dufour and C. Bonnelle, J. Phys. (Paris) **35**, L255 (1974).
[6] F. Gerken, J. Barth, and C. Kunz, Phys. Rev. Lett. **47**, 993 (1981).
[7] J. C. Riviere, F. P. Netzer, G. Rosina, G. Strasser, and J. A. D. Matthew, J. Electron Spectrosc. Relat. Phenom. **36**, 331 (1985).
[8] J. Koaczkiewicz and E. Bauer, Surf. Sci. **273**, 109 (1992).
[9] D. D. Sarma, C. Carbone, R. Cimino, P. Sen, and W. Gudat, Phys. Rev. B **47**, 9199 (1993).
[10] M. Taborelli, R. Allenspach, and M. Landolt, Phys. Rev. B **34**, 6112 (1986).
[11] R. Allenspach, D. Mauri, M. Taborelli, and M. Landolt, Phys. Rev. B **35**, 4801 (1987).
[12] M. Taborelli, R. Allenspach, G. Boffa, and M. Landolt, Phys. Rev. Lett. **56**, 2869 (1986).
[13] C. Carbone and E. Kisker, Phys. Rev. B **36**, 1280 (1987).
[14] T. Kachel, R. Rochow, W. Gudat, R. Jungblut, O. Rader, and C. Carbone, Phys. Rev. B **45**, 7267 (1992).
[15] M. R. Scheinfein, J. Unguris, M. H. Kelley, D. T. Pierce, and R. J. Celotta, Rev. Sci. Instrum. **61**, 2501 (1990).
[16] R. Allenspach, D. Mauri, M. Taborelli, and M. Landolt, Phys. Rev. B **35**, 4801 (1987).
[17] O. S. Anilturk and A. R. Koymen, J. Magn. Magn. Mater. **213**, 281 (2000).
[18] Y. S. Lee, A. R. Koymen, and M. J. Haji-Sheikh, Appl. Phys. Lett. **72**, 851 (1998).
[19] D. E. Ramaker, CRC Crit. Rev. Solid State Mater. Sci. **17**, 211 (1991) and references therein.
[20] E. N. Sickafus, Phys. Rev. **116**, 1436 (1977).
[21] O. S. Anilturk, Ph.D. thesis, The University of Texas at Arlington, 2002.
[22] O. S. Anilturk and A. R. Koymen, J. Appl. Phys. **89**, 7233 (2001).
[23] N. Gryzinski, Phys. Rev. **138**, A338 (1965).
[24] Z. Hu, K. Starke, G. van der Laan, E. Navas, A. Bauer, E. Weschke, C. Schuβler-Langeheine, E. Arenholz, A. Muhlig, G. Kaindl, J. B. Goodkoep, and N. B. Brookes, Phys. Rev. B **59**, 9737 (1999).
[25] J. Sugar, Phys. Rev. B **5**, 1785 (1972).